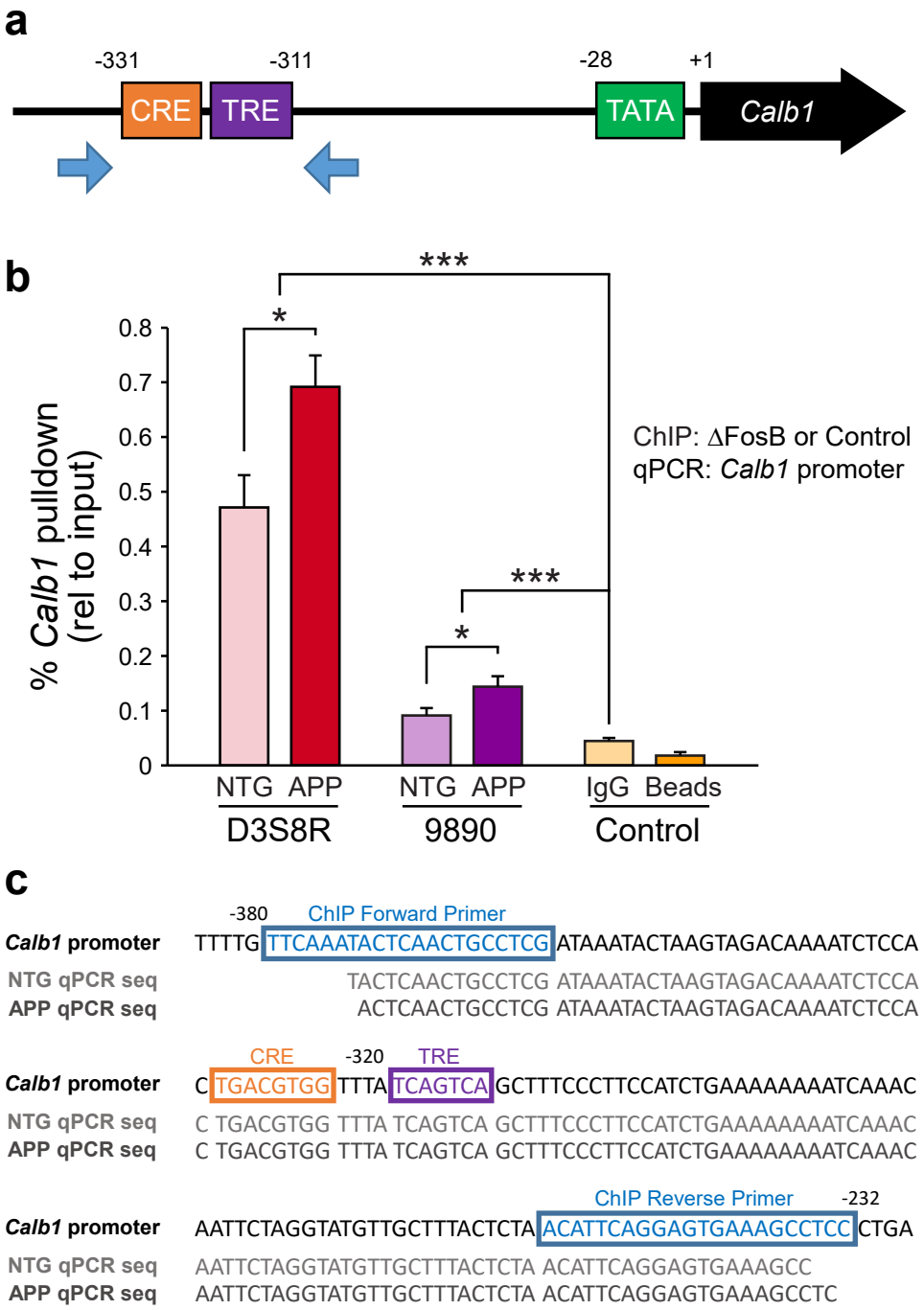

Supplemental Figure 1: Signal-to-noise determination of ΔFosB chromatin immunoprecipitation (ChIP) and *Calb1* promoter pulldown specificity. (**a**) Diagram depicting *Calb1* promoter and location of ChIP primers (blue arrows) used for amplifying CRE and TRE following ΔFosB ChIP on whole mouse hippocampus. (**b**) *Calb1* promoter enrichment (shown as % of input) in ChIP experiments using two different ΔFosB antibodies (D3S8R and 9890) and IgG control (n=8 mice/group; Welch's ANOVA: $F_{5,15.5}$=40.11, p=2.49x10^{-8}; planned comparisons: 9890 vs. IgG ***p=3x10^{-5}, D3S8R vs. IgG ***p=2.28x10^{-9}, 9890 NTG vs. 9890 APP *p=0.042, D3S8R NTG vs. D3S8R APP *p=0.018). Error bars represent SEM. ChIP experiments were performed using the Digital SLP probe sonifier. (**c**) Sequencing of ChIP-qPCR material obtained from ΔFosB ChIP/*Calb1* promoter qPCR in NTG and APP mice.

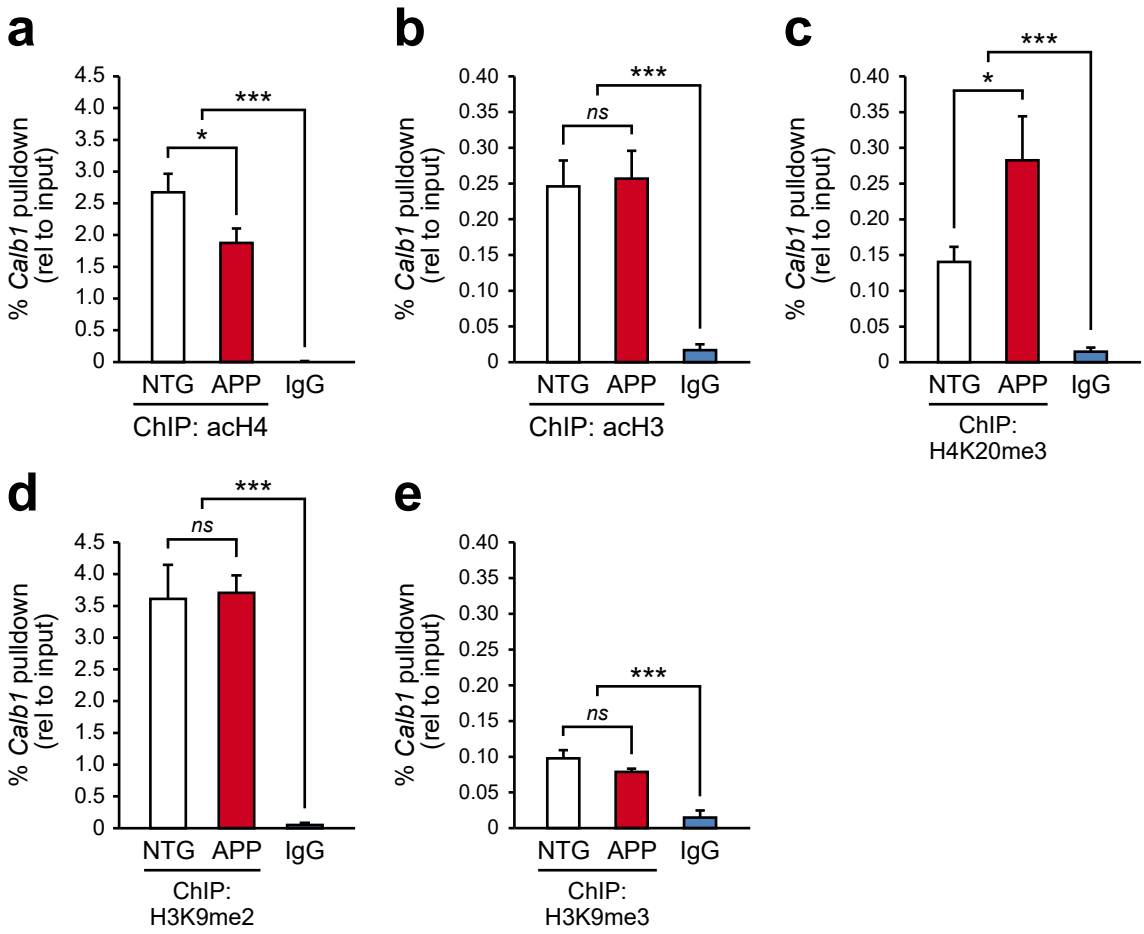

Supplemental Figure 2: Signal-to-noise determination of histone ChIP experiments shown in the manuscript. *Calb1* promoter enrichment (shown as % of input) displayed alongside IgG control ChIPs for (**a**) acetylated histone 4 (Welch's ANOVA: $F_{2,10}$=70.15, p=1x10^{-6}; planned comparisons: NTG vs. APP *p=0.049; acH4 vs. IgG ***p=5.1x10^{-9}), (**b**) acetylated histone 3 (Welch's ANOVA: $F_{2,10.1}$=33.53, p=3.5x10^{-5}; planned comparisons: NTG vs. APP p=0.84; acH3 vs. IgG ***p=2.8x10^{-7}), (**c**) trimethylated histone 4 lysine 20 (Welch's ANOVA: $F_{2,14.4}$=29.02, p=9x10^{-6}; planned comparisons: NTG vs. APP *p=0.032; acH3 vs. IgG ***p=1.2x10^{-5}), (**d**) dimethylated histone 3 lysine 9 (Welch's ANOVA: $F_{2,8.2}$=99.61, p=2x10^{-6}; planned comparisons: NTG vs. APP p=0.88; acH3 vs. IgG ***p=6.9x10^{-7}), (**e**) trimethylated histone 3 lysine 9 (Welch's ANOVA: $F_{2,7.7}$=18.53, p=0.001; planned comparisons: NTG vs. APP p=0.17; acH3 vs. IgG ***p=0.001). ChIP experiments were performed using the Digital SLP probe sonifier. n=4 mice for respective IgG control ChIPs. Histone ChIP sample sizes are reported in Figure 1 of the main manuscript. *ns*, non-significant. Error bars represent SEM.

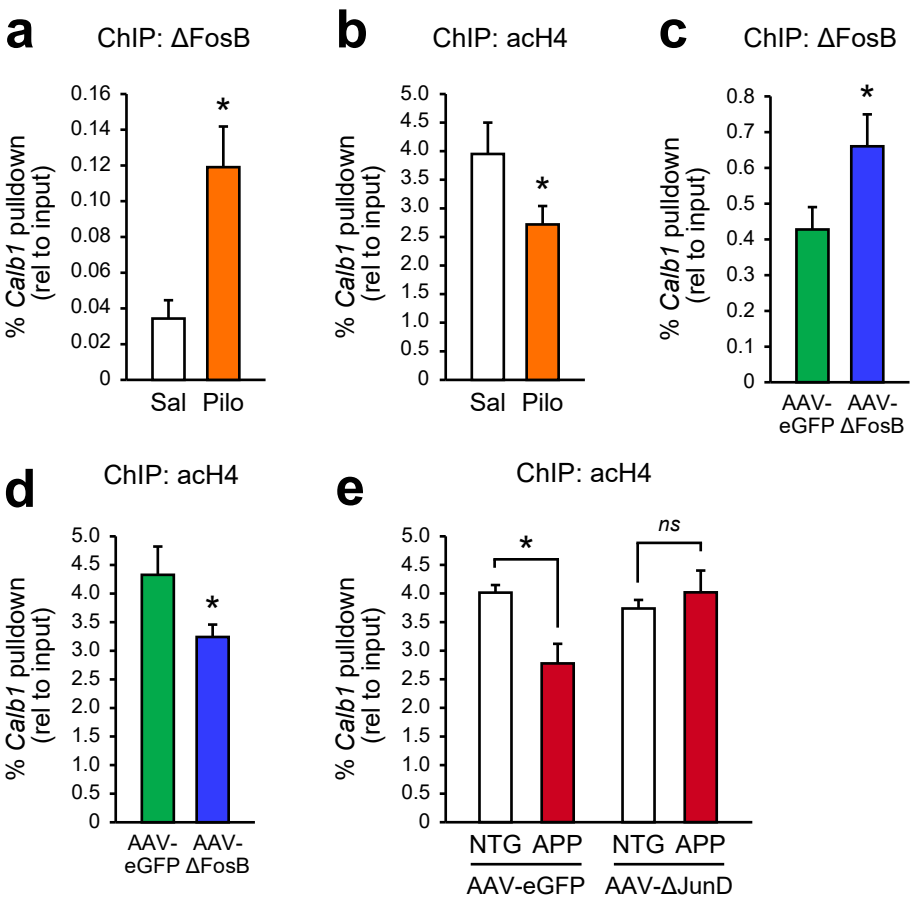

Supplemental Figure 3: Results of ChIP experiments from Figures 1-3 shown as % of input. *Calb1* promoter enrichment for (**a**) ΔFosB in pilocarpine-treated mice (t_6=3.4, **p*=0.015), (**b**) acetylated histone 4 in pilocarpine-treated mice (t_6=-1.94, one-tail **p*=0.05), (**c**) ΔFosB in wild-type mice that received bilaterial hippocampal infusion of adenoassociated virus carrying ΔFosB/eGFP (AAV-ΔFosB) (t_{12}=2.14, **p*=0.05), (**d**) acetylated histone 4 in AAV-ΔFosB mice (t_{12}=-2.21, **p*=0.047), and (**e**) acetylated histone 4 in mice that received bilateral hippocampal infusion of AAV carrying ΔJunD/eGFP (AAV-ΔJunD) (two-way ANOVA: genotype $F_{1,20}$=3.01, *p*=0.098, treatment $F_{1,20}$=3.07, *p*=0.095, interaction $F_{1,20}$=7.656, *p*=0.012; Tukey's HSD: AAV-eGFP/NTG vs. APP **p*=0.022, AAV-ΔJunD/NTG vs. APP *p*=0.88). ChIP experiments for all panels were performed using the Q800R bath sonicator except for panel (c), in which the Digital SLP probe sonifier was used. Sample sizes are reported in the main manuscript. Data in panels (a-d) were analyzed via Student's t-tests. Error bars represent SEM.

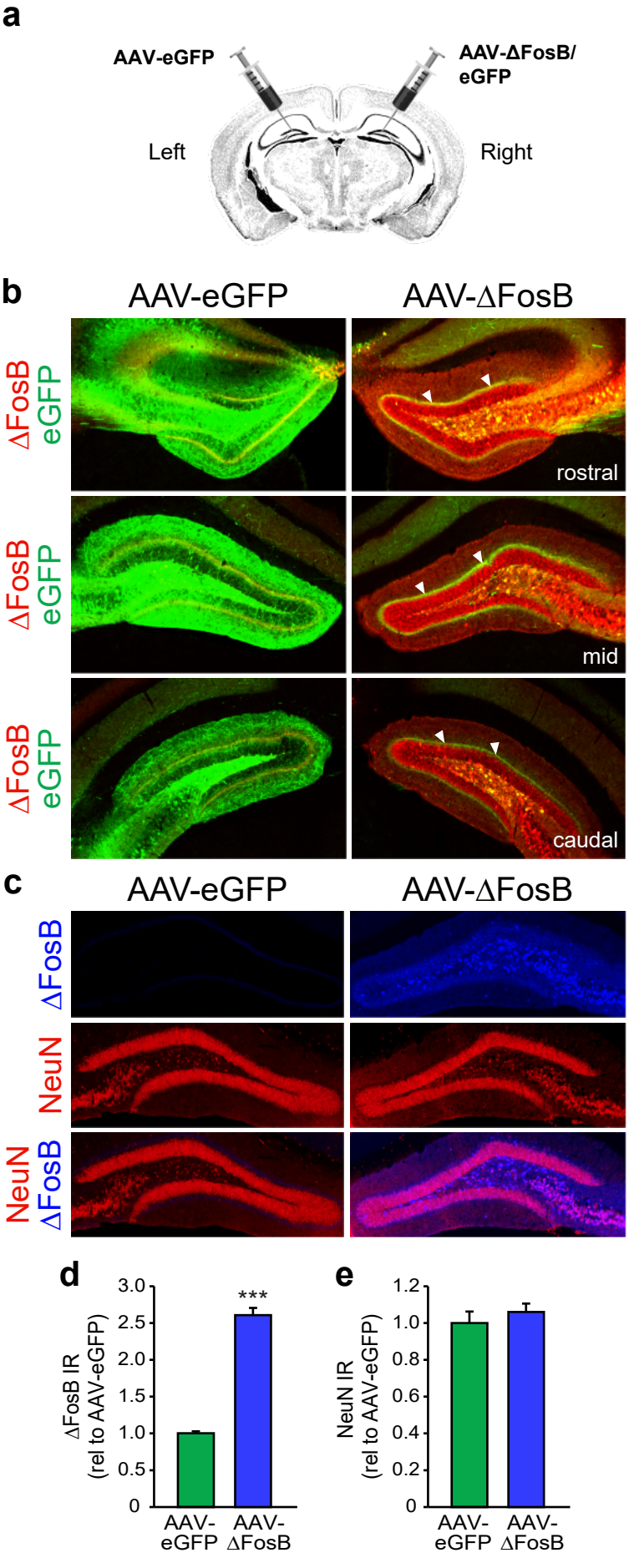

Supplemental Figure 4: Virus-mediated expression of ΔFosB covers the rostral-caudal extent of the dentate gyrus in wild-type mice, and does not impact cell survival or expression of housekeeping genes. (**a**) Virus infusion scheme: adeno-associated virus carrying CMV promoter-driven ΔFosB/eGFP (AAV-ΔFosB) was infused into the right hippocampus of wild-type mice whereas virus carrying eGFP (AAV-eGFP) was infused into the left hippocampus as control. (**b**,**d**) Example images and quantification of ΔFosB immunoreactivity (IR) in the left and right dentate gyri (left and right panels, respectively) of mice that received left-sided AAV-eGFP infusion and right-sided AAV-ΔFosB infusion (n=4 mice/treatment; paired t-test: t_3=17.4, ***p=4.13x10^{-4}). eGFP expression is also shown. Arrowheads denote eGFP-containing projections from the contralateral dentate gyrus. (**c**,**e**) NeuN IR in dentate gyrus granule cells transduced with AAV-eGFP (left panels) or AAV-ΔFosB (right panels) (n=4 mice/treatment; paired t-test: t_3=1.71, p=0.19). Error bars represent SEM.

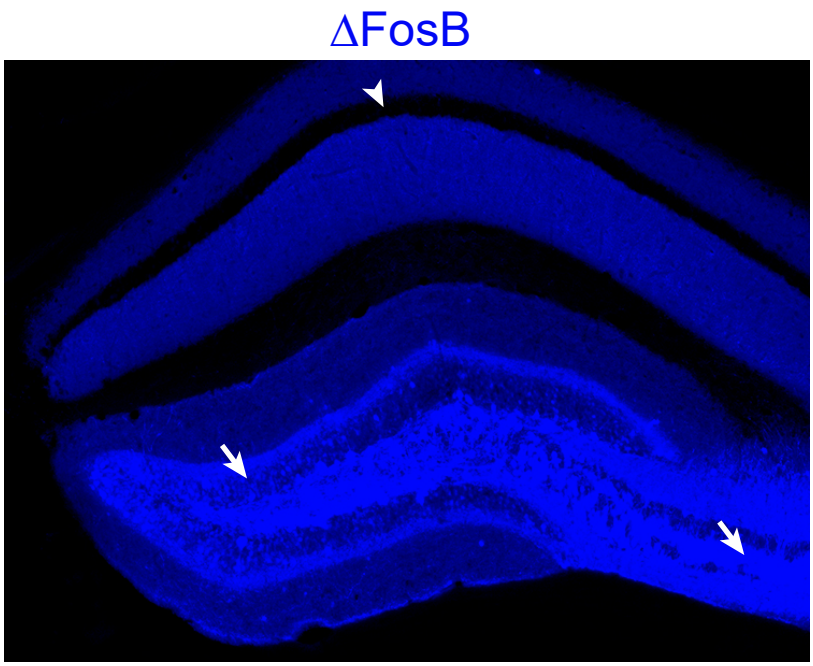

Supplemental Figure 5: Low-magnification image of the hippocampus 28 days after AAV-ΔFosB infusion (related to Figure 2a). Relatively specific ΔFosB expression can be observed in the dentate gyrus and CA3 (arrows), with no expression in CA1 stratum pyramidale (arrowhead). Expression of ΔFosB in CA1 stratum radiatum is due to accumulation of ΔFosB in Schaeffer collateral projections from CA3. Although the CMV promoter drives expression of ΔFosB in both dentate gyrus and CA3, the effects of ΔFosB on calbindin expression are specific to the dentate gyrus as CA3 pyramidal neurons do not endogenously express calbindin.

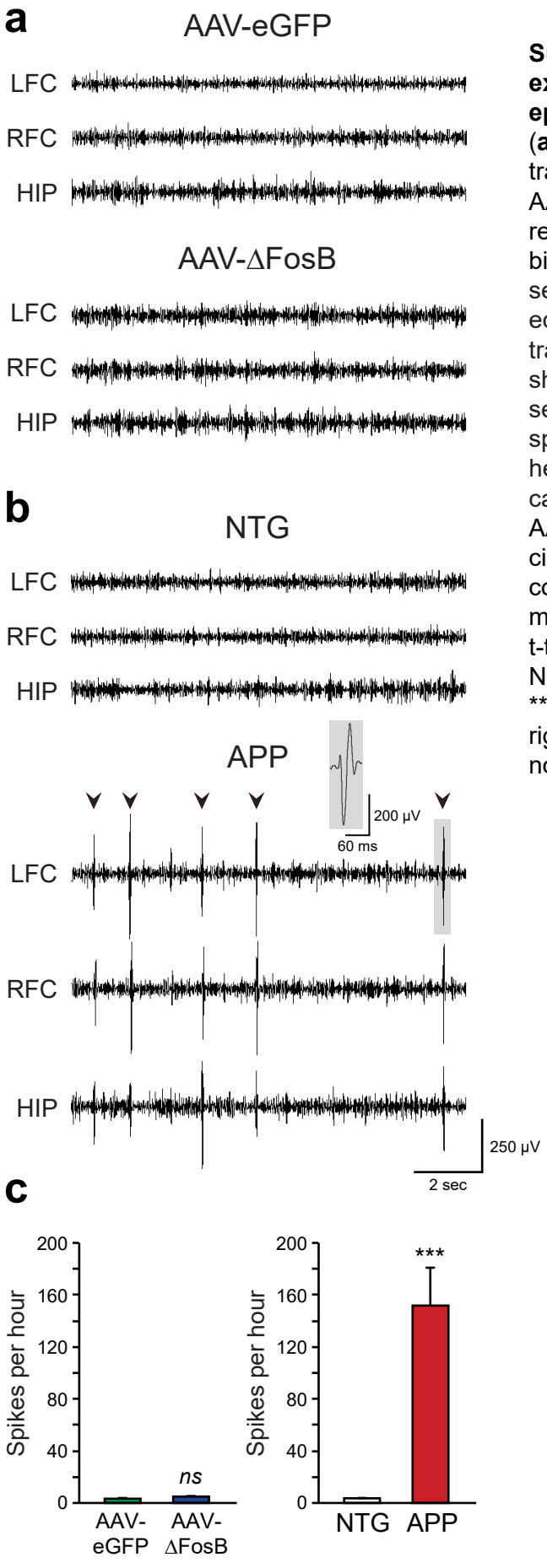

Supplemental Figure 6: Virus-mediated expression of ΔFosB does not generate epileptiform activity in the hippocampus. (**a**) Example electroencephalographic (EEG) traces from wild-type mice treated with AAV-eGFP or AAV-ΔFosB during a 48-hour recording session performed 28 days after bilateral hippocampal virus infusion. No seizures or epileptiform activity were detected after either treatment. (**b**) Example EEG traces from naive NTG and APP mice are shown for comparison. APP mice exhibit seizures (not shown) as well as epileptiform spikes lasting ~60 ms (indicated by arrowheads and magnified in the inset). (**c**) Hippocampal spike frequency in AAV-eGFP versus AAV-ΔFosB mice (left panel). Spike frequencies from NTG and APP mice are plotted for comparison (right panel). AAV-ΔFosB (n=5 mice) vs. AAV-eGFP (n=6 mice) Student's t-test: t_9=1.804, *p*=0.1; APP (n=8 mice) vs. NTG (n=10 mice) Student's t-test: t_{14}=5.109, ***p=2x10^{-4}. LFC, left frontal cortex. RFC, right frontal cortex. HIP, hippocampus. *ns*, non-significant. Error bars represent SEM.

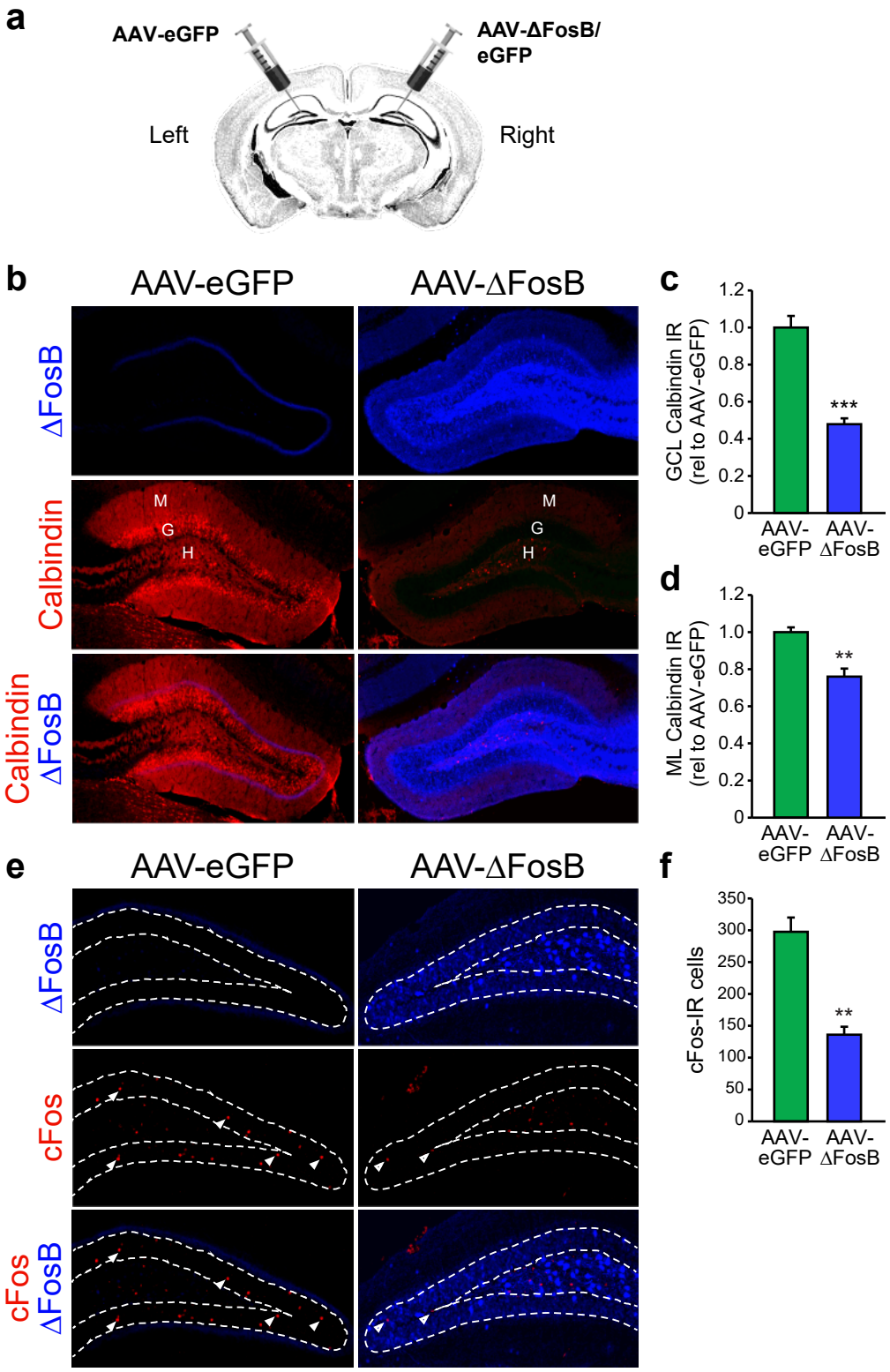

Supplemental Figure 7: ΔFosB suppresses expression of calbindin and cFos in the dentate gyrus. (**a**) Virus infusion scheme: AAV-ΔFosB was infused into the right hippocampus of wild-type mice whereas AAV-eGFP was infused into the left hippocampus as control. (**b**) Images of ΔFosB and calbindin IR in the dentate gyrus after infusion of AAV-eGFP (left panels) or AAV-ΔFosB (right panels). The molecular layer (M), granule cell layer (G), and hilus (H) of dentate gyrus can be observed and correspond to the dendrites, cell bodies, and axons of granule cells, respectively. (**c,d**) Quantification of calbindin IR in the granule cell layer (panel c: n=4 mice/treatment; paired t-test: t_3=-14.2, ***p=7.63x10^{-4}) and molecular layer (panel d: n=4 mice/treatment; paired t-test: t_3=-6.67, **p=0.0069). (**e**,**f**) Images and quantification of cFos IR in the dentate gyrus after infusion of either AAV-eGFP (left panels) or AAV-ΔFosB (right panels) (n=4 mice/treatment; paired t-test: t_3=-9.56, **p=0.0024). Dotted lines denote the boundaries of the granule cell layer in panel (e). Arrowheads, cFos-IR cells. Error bars represent SEM.

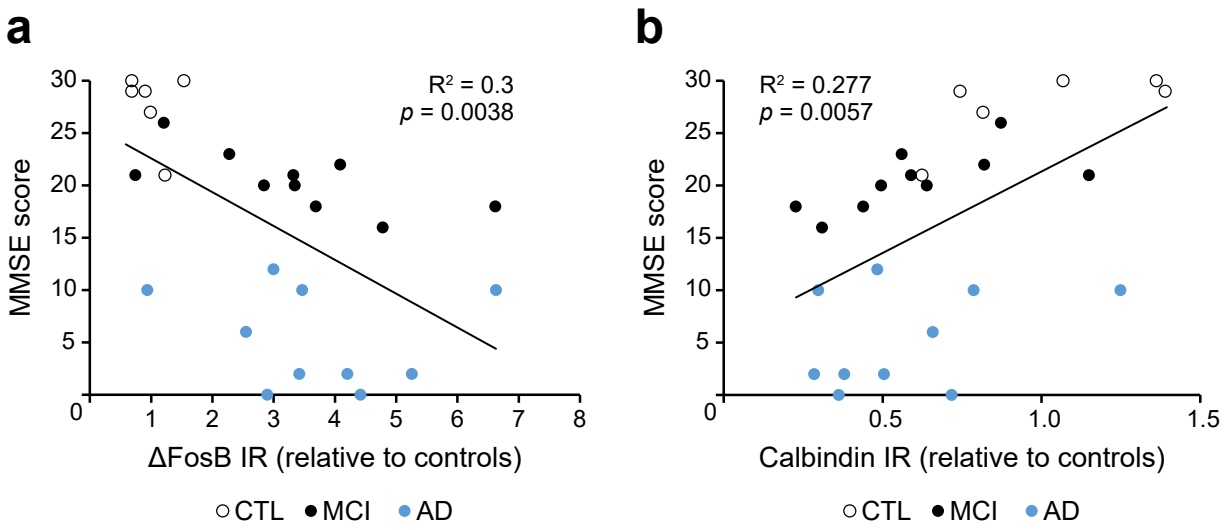

Supplemental Figure 8: Increased ΔFosB expression and decreased calbindin expression in the dentate gyrus of human patients correlate with cognitive deficits (n=26 patients). MMSE, Mini-Mental State Examination. CTL, control. MCI, mild cognitive impairment.

a

Diagnosis	MMSE	Age	Sex	Braak Stage
Control	30	94	M	2
Control	29	87	M	1
Control	21	69	M	0
Control	29	91	M	3
Control	30	63	F	1
Control	27	79	F	0
MCI	26	88	M	6
MCI	20	77	M	6
MCI	18	74	M	6
MCI	16	73	F	6
MCI	20	76	F	6
MCI	22	56	M	6
MCI	21	79	F	6
MCI	21	71	M	6
MCI	23	67	M	5
MCI	18	79	F	6
AD	10	66	F	6
AD	12	74	F	6
AD	0	71	F	6
AD	10	70	F	6
AD	6	64	F	6
AD	0	65	F	6
AD	10	75	M	6
AD	2	61	M	6
AD	2	57	F	6
AD	2	78	M	6

b

Diagnosis	Age	Sex	Pathology
TLE	60	F	Hippocampal sclerosis
TLE	38	F	Hippocampal sclerosis
TLE	43	M	Hippocampal sclerosis
TLE	32	M	Hippocampal sclerosis
TLE	55	F	Hippocampal sclerosis
TLE	43	F	Hippocampal sclerosis
TLE	33	F	Hippocampal sclerosis
TLE	38	F	Hippocampal sclerosis

Supplemental Figure 9: Available patient information for (a) fixed dentate gyrus samples from postmortem control, MCI, and AD patients and (b) hippocampal resection specimens from temporal lobe epilepsy (TLE) patients. Controls for MCI and AD are defined by normal cognitive scores on clinical exams and/or lack of AD-related pathology in the hippocampus.